

Design and implementation of Schumann resonances sensor platform

C. I. Votis^{1,*}, G. Tatsis¹, V. Christofilakis¹, P. Kostarakis¹, V. Tritakis² and Ch. Repapis²

¹Physics Department Electronics-Telecommunications and Applications Laboratory University of Ioannina, Ioannina, Greece

²Marionopoulos-Kanaginis Foundation for the Environmental Sciences, Athens, Greece

Received 30 June 2015; Accepted 25 October 2016

Abstract

The principal objective of this paper is to present a Schumann resonances detection and measurements platform. Studies and investigation on Schumann resonances are suggested in several research activities that aim to monitor climate, earth and atmospheric phenomena. Schumann oscillations are natural electromagnetic eigenmodes at ELF frequency range. Design and implementation of the proposed platform are based on principal theoretical considerations and laboratory observations including initialization, test measurements and calibration. The proposed measurement platform is an efficient and versatile set-up for experimental detection and measurements on Schumann resonances magnetic field components. Several preliminary outdoor measurements have already conducted, providing principal results that ensure efficient and reliable performance.

Keywords: Inductor coil sensor, Magnetic field component detection, operational amplifier, active filter circuit, Telecommunications

1. Introduction

Earth-ionosphere cavity is an electromagnetic cavity that exhibits its resonant modes in the ELF and ULF ranges. The Schumann resonances (SR) are quasi-standing electromagnetic waves in that cavity at ELF frequencies 7.8, 14, 20, 26, 33, 39, and 45 Hz. These standing waves are provided mainly by thunderstorm activities as a result of resonance between direct and round the world ELF waves. Observations from short and long term monitoring of the Schumann phenomena are recently greatly important and interesting mainly in the field of geophysics. Schumann resonances detection is a complex procedure that involves measurements of the limited energy generated and dissipated by the global lighting activity inside the huge volume of Earth-ionosphere cavity. That smeared total energy provides vertically oriented prevailed electric component with amplitude that approximates to 10^{-7} V/m. The corresponding two magnetic field components are horizontal at N-S and E-W orientation with amplitudes of several tenths of pT. The proposed measurement platform is an efficient and versatile induction sensor system for Schumann magnetic field detection applications. That set-up consists of an inductor coil and a signal conditioning system, providing ELF signal range collection of the magnetic field energy from Schumann resonance standing waves [1-4].

Design and implementation aspects of the proposed inductor coil sensor for Schumann resonance detection applications are included in Section 2 and 3. The architecture of the proposed induction coil structure are presented and discussed in Section 2. The signal conditioning system is in detail presented and described in Section 3. Resultant data from preliminary SR magnetic field components measurements are also presented in Section 3. The article concludes to Section 4.

2. Inductor coil architecture

Magnetic field antenna architecture we designed and implemented is based on an inductor coil with a ferromagnetic core material. That material exhibits relative magnetic permeability of the order of 10^5 , providing considerable antenna sensitivity enhancement using practical number of turns and range of cross section area. The proposed antenna uses a mumetal core that relates to mumetal ASTM A753 Alloy 4 specification and provide quite $2 \cdot 10^5$ magnetic permeability. A rod (length 300 mm & diameter 25 mm) of that mumetal material was used as the core of the proposed antenna inductor coil. Table 1 presents the geometry parameters values that are involved in the proposed inductor coil geometry.

Table 1. Inductor coil geometry

Geometrical parameter	Value
l _{core} /l _{winding}	300 mm / 250 mm
d _{core}	25 mm
d _{wire}	0.25 mm

The mumetal core material was installed in our inductor winding machine in order to construct quite 40000 turns using a copper wire of 0.25 mm diameter. The resultant antenna inductor coil performance depends on several parameters that relate to a fundamental factor named as demagnetization factor (N). The length of the windings we implemented meets an important requirement that determines the windings coverage on the mumetal rod surface. In fact, the copper wire windings should cover the 70 % to 90 % of the total core length turns so that the magnetic flux we achieved exhibits quite maximum value. Also, the choice of the extra high magnetic permeability core material ensures significant antenna inductor coil performance enhancement. That is because the magnetic permeability of the proposed antenna structure has no dependence on the magnetic characteristics of the mumetal core material. As a result, the apparent magnetic

* E-mail address: kvotis@grads.uoi.gr

permeability (μ_{app}) of the proposed antenna inductor coil has a strong dependence on demagnetization factor. That parameter relates to inductor coil geometrical characteristics and mainly depends on the ratio of the core length to core diameter value (m). Equations 1 and 2 describe the demagnetization factor and the apparent magnetic permeability of the proposed antenna inductor coil [5, 6].

$$N = \frac{1}{m^2} \cdot [\ln(2 \cdot m) - 1] \quad (1)$$

$$\mu_{app} = \frac{1}{N} \quad (2)$$

Using the key values that are included in Table 1 and employing equation 1 the resultant demagnetization factor approximates to 0.0151. The value of the apparent magnetic permeability of the proposed inductor coil is then derived by equation 2 (close to 66). As already mentioned, the value of μ_{app} is of great importance because has a strong influence on the proposed magnetic field antenna performance. That influence refers not only through the induced voltage (Vi) in the inductor coil terminals but also through other critical parameters that relates to the inductor coil geometry. In fact, principal theoretical aspects indicate that the inductor coil structure exhibits self-capacitance, self-inductance and self-reactance, providing an equivalent RLC circuit [7,8]. Those parameters exhibit strong dependence on the value of the apparent magnetic permeability. Table 2 includes the calculated and measured values of the inductor coil circuit reactance and inductance. The self- capacitance was only experimentally measured.

Table 2. Inductor coil equivalent circuit parameters values

	Calculated	Measured
Resistance R	1548 Ω	1560 Ω
Inductance L	233 H	249 H
Capacitance C	-	440 pF

From those results, the calculated values exhibit quite small declinations from the corresponding measured values. As the proposed inductor coil is typically an ELF magnetic field antenna, an electrostatic shield is necessary in order to eliminate coupling effects induced by electric field components that may co-exist in the measurement set-up environment. In that way, the proposed inductor coil implementation is installed inside a wooden box using foam components. The outer face of the box is covered by an unmagnetic material sheet (copper) for electromagnetic shielding purposes. Inside the wooden box, the distance between the inductor coil and the inner face of the box ensures elimination of coil capacitance distortion and noise contribution. Figure 1 depicts the proposed inductor coil antenna implementation inside the wooden box.

3. Signal conditioning system architecture

Principal aspects on Schumann resonances studies demonstrate that the signal conditioning system has a key role in the magnetic field sensor performance and efficiency. As the induced voltage amplitude at the inductor coil terminals exhibits quite extra low values (several tenths of nVolts), the proposed sensor platform should meet all the

corresponding requirements in signal conditioning applications for better noise performance and less signal distortion and degradation. In fact, the signal conditioning system should embody a multiple stage amplifying and filtering circuitry in cascading topology, providing remarkable performance and efficiency at extra low values voltage input and at frequency range of DC to 60 Hz. The architecture of the proposed signal conditioning system is based on operational amplifier circuitry that offer a wide range of applications at signal amplification and filtering [9]. One of the fundamental aspects on operational amplifier performance is noise elimination. Evaluating such parameter both internal and external noise sources should be considered. Employing the simplified equivalent circuit and considering that the noise sources are uncorrelated we calculated the total noise referred to the input for several operational amplifier ICs through equation 3.



Fig.1. Installation of the inductor coil

$$V_{ni} = \sqrt{e_n^2 + (R_s \times i_n)^2 + V_n(R_{out})^2} \quad (3)$$

where e_n and i_n are the input referred voltage and current noise, the R_s is the input resistance of the operational amplifier topology and $V_n(R_{out})$ is the voltage noise from external circuitry (R_1 and R_2) [10]. Such calculations are based on operational amplifiers performance parameters, considering that the external circuitry exhibits 1500 Ω resistance. Also, the noise bandwidth ranges from 1 to 35 Hz. The resultant values for the most effective operational amplifiers in terms of total noise are presented in Table 3 [11-15].

Table 3. Operational amplifier Noise performance

Opamp	En (nVolts)	In (pA)	Vni (nVolts)
OPA209	3.3	0.6	6.04
ISL28127	3.2	1	6.11
AD8671	2.0	1.4	5.77
OPA27/37	3.8	1.7	6.77
OP27	3.5	1.7	6.60

Based on those results, it seems that OPA209 is a precision operational amplifier that provides quite excellent noise performance. The other operational amplifiers exhibit quite extra small declination from such performance. For more efficient and low noise performance on the proposed sensor platform signal conditioning system, we chose the OPA209 operational amplifier for the first amplifying stage and the AD8671 for the others stages. In fact, the proposed Schumann resonances sensor platform is based on a signal conditioning system that consists of eight amplifying and filtering stages.

The preamplifier - first stage is a non-inverted operational amplifier circuitry that embodies a RC single pole high pass filter for flicker noise degradation. Also, there is a double choice on feedback equivalent impedance for full-scale or semi-scale amplification. That preamplifier circuitry is installed inside the wooden box and close to the inductor coil for better noise performance. From the frequency response measurements, it is obvious that the passband gain value approximates the value of 30 dB or 17 dB at a frequency range from 1 Hz to 100 Hz depending on high or low level amplification.

The second stage in the proposed cascading topology is a combination of a Sallen-key second order low pass filter and a 50 Hz Twin – T notch filter [16]. That second stage performance mainly aims to eliminate 50 Hz signal component from household power system. It also exhibits a quite no ripple passband gain at frequency range from 1 Hz to 24 Hz.

The third, fourth and sixth stage at the proposed signal conditioning system depend on Sallen Key fourth order low pass filter topology [16]. Both those circuitries exhibit frequency responses that degrade signal amplitudes with frequency values higher than 25 Hz. The total passband gain value approximates to 35 dB. For further flicker noise degradation, we also used a Sallen-key second order high pass filter at the fifth stage on the cascading stages signal conditioning system. That circuitry stage exhibits a no ripple 14 dB passband gain at a frequency range of 1 Hz to 100 Hz. Also, the cut off frequency value approximates to 1.8 Hz so that the flicker noise degradation is achieved.

The next stage at the proposed signal conditioning system is based on non-inverted operational amplifier topology with adjustable gain values ranges from 0 to 26 dB. Also, two identical RC single pole high pass filters are installed at the input and output of that stage for flicker noise degradation.

The last stage consists of a Sallen-Key fourth order bandpass filter. The frequency response experimental results indicate that the last stage has passband frequency range from 3 Hz to 28 Hz and a total passband gain 8 dB. Using the laboratory equipment, we also measured the total frequency response at second to eighth cascading stages. The resultant measurements are presented in Figure 2.

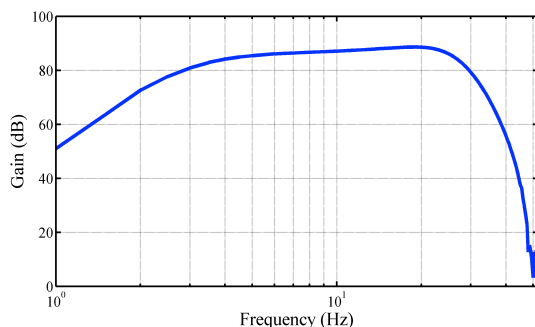


Fig. 2. Experimental frequency response of 2nd to 8th stages

The form of that curve indicates that the total passband gain of the 2nd to 8th stages of the proposed signal conditioning system approximates the value of 90 dB at 10 Hz. Also, the gain value variations for the signal frequency values upper the limit of 50 Hz are mainly provided by the laboratory calibration device which exhibits limited performance at a frequency range of 40 Hz to 100 Hz.

Apart from the first stage of the proposed cascaded signal conditioning system, all other stages are installed inside a

metallic box for EMI shielding purposes. Using the inductor coil with the preamplifier stage at the wooden box along with the cascading stages at the metallic box we made a course of preliminary measurements in order to achieve detection and recording of Schumann resonances at an outdoor area close to the Araxthos River in Ioannina, Greece. At those experimental measurements, the main axis of the inductor coil is aligned with the prevailing magnetic field horizontal component (N-S) [4]. Using a collection of stored and recorded 10 min duration samples and employing mathematical manipulation we then calculated the corresponding power spectrum density. Figure 3 shows the results at a frequency domain.

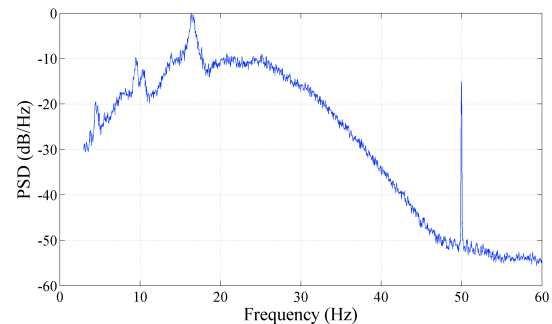


Fig. 3. Power spectrum density of Sensor output signal

Those preliminary results indicate that there are a number of signal components with frequency values that relate to the first (fundamental), and harmonics Schumann resonances components. Those results also present a quite low level signal component that corresponds to the 50 Hz signal of the household power system. That signal could be a pilot signal component ensuring efficient and reliable performance of the proposed Schumann sensor platform. Also those results demonstrate that the whole implementation has been experimentally tested, giving remarkable performance and considerable signal sampling and detection efficiency.

4. Conclusion

An inductor coil sensor platform for Schumann resonances detection applications was in detail presented and discussed. The proposed architecture introduces an inductor coil implementation for magnetic field components detection at ELF range. Both inductor self-parameters and signal detection performance were studied and investigated in terms of efficiency. Signal conditioning system of the proposed sensor platform was also presented and discussed through extended noise analysis and a course of experimental test measurements. The inductor coil implementation and the signal conditioning system are installed at outdoor environment in order to achieve signal samples time acquisition. Based on those measurements, the power spectrum density of the complex signal is calculated using mathematical tools and methods. Summarizing the experimental power spectrum results, it is concluded that the proposed system represents an efficient and versatile experimental platform for Schumann resonances detection and recording applications.

This paper was presented at Pan-Hellenic Conference on Electronics and Telecommunications - PACET, that took place May 8-9 2015, at Ioannina Greece.

References

1. Kristian Schlegel and Martin Fullekrug, "50 years of Schumann resonances", *Physik in unserer Zeit*, 33(6), 256 – 26, 2002. Translation Catarina Geoghan, 2007
 2. Colin Price, Olga Pechony and Eran Greenberg, "Schumann resonances in lighting research", *Journal of lighting research*, Vol. 1, 2007, pp. 1 -15
 3. Fernando Simoes, Robert Pfaf and Henry Freudenreich, "Observation of Schumann resonances in the Earth Ionosphere", NASA/ Goddard Space Flight Center, Greenbelt, MD 20771 USA
 4. A. Ondraskova, S. Sevcik, L. Rosenberg, P. Kostecky, L. Turna and L. Kohut, "The detection of magnetic field component of Schumann eigenmodes using search coil sensors at Modra observatory", *Measurements science review*, Vol. 5, section 3, 2005
 5. Slawomir Tumanski, "Induction coil sensors – a review", Institute of Physics publishing, measurement science and technology, 18, 2007, pp 31 - 46
 6. A.V. Shvets, "The analysis of magnetic search – coil antenna of high sensitivity and small dimensions", Usikov Institute of Radiophysics and Electronics, Ukrainian National Academy of Sciences
 7. Steven A. Macintyre, "Magnetic Field Measurement", 1999 CRC Press LLC
 8. Kevin Kuang, "Magnetic Sensors – Principles and Applications", InTech, 09 March 2012, 160 pages
 9. Malvino A. "Electronics principles" Tata McGraw Hill, 2006
 10. AN-940 Application note, Analog Devices
 11. OPA 209 Datasheet, Texas instruments, October 2013
 12. ISL28127 Datasheet, Linear Technologies, December 16, 2010
 13. AD8671 Datasheet, Analog Devices, Ref. F
 14. OPA27/37 Datasheet, Texas Instruments, August 2005
 15. OP27 Datasheet, Analog Devices, Rev. C
- S. Winder, "Analog and Digital Filter Design", Newnes, 2002F.D Galiana, K Almeida, "Assessment and control of the Impact of FACTS devices on power system performance", IEEE Transactions on power systems, Vol .II, No 4, pp1931- 1936, November 1996.